Research paper

Optical properties of Eu(III) and Tb(III) complexes with pyridine- and quinoline- based ligands under high hydrostatic pressure

Fabio Piccinelli[a,*], Chiara De Rosa[a], Agata Lazarowska[b], Sebastian Mahlik[b], Marek Grinberg[b], Takayuki Nakanishi[c], Shun Omagari[d], Marco Bettinelli[a]

[a] *Luminescent Materials Laboratory, Dipartimento di Biotecnologie, Università di Verona and INSTM, UdR Verona, Strada Le Grazie 15, 37134 Verona, Italy*
[b] *Institute of Experimental Physics, Faculty of Mathematics, Physics and Informatics, University of Gdańsk, 80-308 Gdańsk, Poland*
[c] *Department of Materials Science and Technology, Faculty of Industrial Science and Technology, Tokyo University of Science, 6-3-1, Niijuku, Katsushika-ku, Tokyo 125-8585, Japan*
[d] *Department of Materials Science and Engineering, School of Materials and Chemical Technology, Tokyo Institute of Technology, 2-12-1, Ookayama, Meguro-ku, Tokyo 152-8552, Japan*

ABSTRACT

The spectroscopy of nitrate complexes of Eu(III) and Tb(III) with chiral and racemic imine-based [**L1** = (N,N'-bis (2-pyridylmethylidene)-1,2-(R,R + S,S)-cyclohexanediamine) and **L3** = N, N'-bis(2-quinolylmethylidene)-1,2-(R,R + S,S)-cyclohexanediamine] and amine-based [**L2** = N,N'-bis(2-pyridylmethyl)-1,2-(R,R + S,S)-cyclohexanediamine) and **L4** = N,N'-bis(2-quinolylmethyl)-1,2-(R,R + S,S)-cyclohexanediamine] ligands has been studied under high hydrostatic pressure (above 100 kbar). With the increasing pressure, a reduction of the Tb(III) and Eu(III) luminescence intensity is detected for all the complexes, whilst a significant reduction of the Tb(III) and Eu(III) excited state lifetimes has been observed for all Tb-based complexes [**L1**Tb(NO$_3$)$_3$ → **L4**Tb(NO$_3$)$_3$] and only for the Eu(III) complexes containing the imine-based ligands [**L1**Eu(NO$_3$)$_3$ and **L3**Eu(NO$_3$)$_3$]. This behavior has been rationalized taking into account two main aspects: i) the relative position of the energy levels of the ligands and the metal ions and ii) the change of these position upon compression DFT calculations have been also performed to elucidate the nature of the orbitals involved in the UV electronic absorption transitions (NTO orbitals) upstream of the energy transfer process to the metal ion.

1. Introduction

Luminescent complexes of lanthanide ions play a pivotal role in a multitude of applications, for example in the field of bioimaging and sensing [1–6], for technological applications such as organic emitting layers in light-emitting diodes (OLED) [7–10] and as solar concentrators [11–13]. In all cases, a strong overall luminosity or brightness (B) is required. As B = ε·ϕ, with ε molar absorption coefficient and ϕ the luminescence quantum yield, sizable brightness values are expected if the ligand strongly absorbs the exciting light and efficiently transfers the excitation energy to the lanthanide ion (*antenna effect*). The energy gap between the donor and acceptor levels is one of the most important factors affecting the efficiency of *antenna effect*. Acceptor levels are the excited states of lanthanide ions (f*). Due to the shielding of the 4f electrons from the environment by the outer complete 5 s and 5p shells, the 4f levels of the lanthanide ion are essentially "fixed" relative to the ground state. On the other hand, the donor

electronic levels, localized on the organic ligand, are strongly dependent on its nature. Therefore, a fine tuning of the electronic structure of the *antenna* molecule is often performed in order to optimize the ligand to metal energy transfer [14].

Another (less investigated) possibility to tune the energy gap between the donor and acceptor levels is to act on the hydrostatic pressure in the solid state materials. High pressure has a significant influence on the singlet and triplet levels of the ligands, whereas the 4f levels are much less sensitive to compression. Therefore, the efficiency of the energy transfer from the triplet state to the 4f levels can be tuned by applying an external pressure on the lanthanide complexes in the solid state. This has been nicely documented for β-diketonate complexes of Eu(III)(III), Tb(III)(III) and Sm(III)(III) [15]. Tuning the energy levels of the ligands with pressure is comparable to studying a series of ligands with different positions of the energy levels. The changes of the emission intensity and of the decay time with pressure can help us to elucidate several details of the energy transfer process (i.e. the nature of

the Ln(III)(III) acceptor level, the presence of CT states, etc.).

In the present contribution, we study the effect of the hydrostatic pressure on the luminescence features of Tb- and Eu-based complexes. In order to have available extensive case studies, we employed ligands possessing different energy positions of the donor levels (i.e. singlet and triplet states). This is possible thanks to the presence of different heteroaromatic *antennae* (pyridine in ligands **L1** and **L2**; quinoline in the ligands **L3** and **L4**, Fig. 1), which furthermore can be conjugated to an
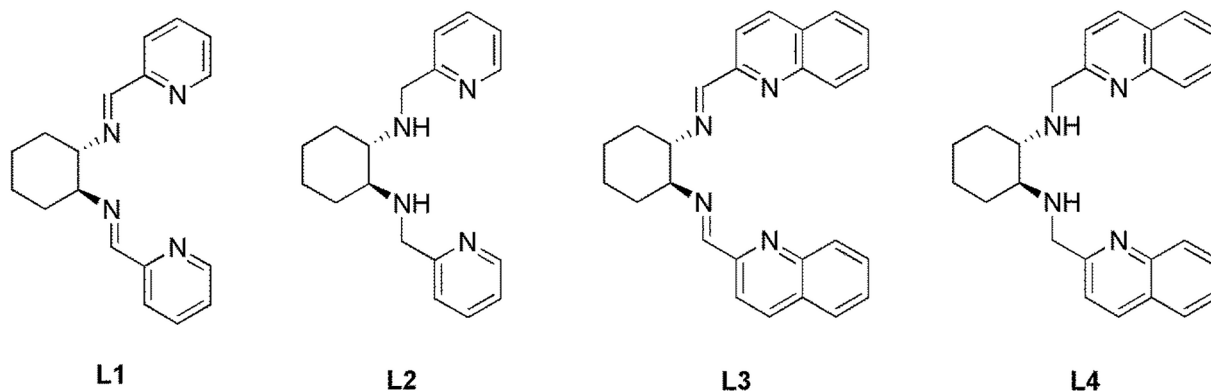
without frozen-core potentials. Natural transition orbitals were calculated from the excited states calculations [20].

3. Results and discussion

3.1. DFT calculations

The structure of the ligands used for this study are depicted in Fig. 1.

Fig. 1. Molecular structure of the ligands discussed in this paper.

imine functional group (ligands **L1** and **L3**, Fig. 1). Density Functional Theory (DFT) calculations have been also employed to clarify the nature of the orbitals involved in the main UV absorption transitions. Conclusions have been also drawn to discuss the role of the pressure on the energy positions of the donor levels localized on the ligands.

2. Experimental

The synthesis of the ligands and relative Tb(III) and Eu(III) complexes has been already reported in the literature [16,17]. Conventional luminescence emission and excitation spectra were recorded using a FluoroMax-4P Horiba Jobin-Yvon spectrofluorimeter. The experimental setup for the luminescence kinetics and time resolved spectroscopy consists of a PL 2143 A/SS laser pumping a PG 401/SH parametric optical generator that generates 30 ps pulses of tuned wavelength with frequency 10 Hz. The detection part consists of a 2501S (Bruker Optics) spectrograph and a Hamamatsu C4334- 01 Streak Camera. Time resolved luminescence spectra were collected by integration of the streak camera pictures over the time intervals, whereas luminescence decays were collected by integration of the streak camera pictures over the wavelength intervals. The experiments at high pressures were carried out using the latter spectroscopic equipment, together with a Merrill-Bassett type diamond anvil cell (DAC). Poly (dimethylsiloxane) oil was used as the pressure-transmitting medium, and a ruby crystal was used as the pressure detector. All the measurements were carried out at room temperature.

The geometries of the lanthanide complexes were optimized using density functional theory (DFT) with CAM-B3LYP functional [18] in the Gaussian09 Revision D.01 program package [19]. The lanthanide ion was replaced with Y atom to simplify the calculations. Starting geometry for the optimization was those taken from the single-crystal X-ray crystallography, except for **L4**Y(NO$_3$)$_3$ in which **L2**Y(NO$_3$)$_3$ with additional aromatic rings was used. The complexes were roughly optimized using 3-21G basis set, and then further optimized using combinatory basis sets of 6-31 + +G(d,p) for C, H, N, and O atoms and SDD (effective core potentials) for Y atom. To ensure that the structure optimized on the minima of the potential-energy surface, analytical vibrational frequencies have been calculated. No imaginary frequency was found in any of the optimized structures. Excited states were calculated using time-dependent density functional theory (TD-DFT) for 10-singlet states

On the basis of the available crystal structures of **L1**Eu(NO$_3$)$_3$, **L2**Eu (NO$_3$)$_3$ [22] and **L3**La(NO$_3$)$_3$ [17] we performed a DFT structural optimization upon substitution of lanthanide ion with Y(III), which is much easier to model from a computational point of view (Fig. 2). The calculated structure of **L2**Y(NO$_3$)$_3$ is in practice superimposable to the experimental one of **L2**Eu(NO$_3$)$_3$, whilst in **L1**Y(NO$_3$)$_3$ and **L3**Y(NO$_3$)$_3$ the aromatic rings were more twisted than in the crystal structures of Eu and La analogs. We postulate that the conjugation of bridging nitrogen atom played a pivotal role in producing the twisting structure because the atom is not conjugated for **L2**Y(NO3) while **L1**Y(NO$_3$)$_3$ and **L3**Y(NO$_3$)$_3$ is. This is further supported with the result of **L4**Y(NO$_3$)$_3$ that showed similar structure with that of **L2**Y(NO$_3$)$_3$.

The energy of the molecular orbitals of the complexes are shown in Fig. S1, together with their most relevant calculated wavelengths of absorption in the UV electronic spectra (Table S1).

Here, we focus on the lowest strong absorption transitions, namely S$_0$-S$_5$ [**L1**Y(NO$_3$)$_3$ and **L2**Y(NO$_3$)$_3$] and S$_0$-S$_3$ [**L3**Y(NO$_3$)$_3$ and **L4**Y (NO$_3$)$_3$]. Numerous molecular orbitals contributed to the transitions, and it was not clear as to what orbitals were truly involved. We therefore employed natural transition orbitals (NTO) calculations that offer simple representation of the transition density between the ground and the excited state. From the inspection of Fig. S2, one can clearly see that the orbitals involved in the lowest strong absorption transitions are in all cases located in the heteroaromatic fragments (pyridine or quinoline) so that this absorption can be considered a locally-excited (LE) transition.

From Table S1, it is possible to draw the UV absorption spectra of the complexes (Fig. S3). They are all qualitatively consistent with the experimental ones [16,17]. As expected, upon extension of the conjugated π electronic cloud the energy gap of the lowest absorption band decreases. This is the case when the imine group is conjugated to pyridine and quinoline rings, in the **L1**Y(NO$_3$)$_3$ and **L3**Y(NO$_3$)$_3$, complexes.

3.2. Luminescence spectroscopy

3.2.1. Pyridine-based complexes

Luminescence excitation spectra complexes are presented in Fig. 3 (a). The luminescence excitation spectra of **L1**Eu(NO$_3$)$_3$ and **L2**Eu (NO$_3$)$_3$ are monitored at 620 nm that corresponds to the $^5D_0 \rightarrow {}^7F_2$ transition in Eu (III). The spectrum of **L2**Eu(NO$_3$)$_3$ consists of a sharp

lines associated with the f-f transitions from the ground state to the excited states of Eu(III) ion and a broadband with maximum at about 280 nm and which covers a wide range of wavelengths (230–320 nm). This band is superimposable to the one observed in the diffuse reflectance spectra of the relative Ln complexes (Ln = La, Gd and Lu) [16]. The spectrum of **L1**Eu(NO$_3$)$_3$ differs from **L2**Eu(NO$_3$)$_3$ with the presence of an additional band at 320 nm. The luminescence excitation spectra of **L2**Tb(NO$_3$)$_3$ and **L1**Tb(NO$_3$)$_3$ are monitored at 545 nm corresponding to the $^5D_4 \rightarrow {}^7F_5$ transition in Tb(III). The spectrum consists of a sharp lines associated with the f-f transitions from the ground state to the excited states of Tb(III) ion and broadband with maximum at about 300 nm. In the case of **L1**Tb(NO$_3$)$_3$ and additional broad band with maximum about 330 nm is observed. The qualitative accordance between the experimental and calculated electronic spectra of **L1** and **L2**-based Ln complexes allow us to conclude that the transition related to the orbitals located on the aromatic moieties of the ligands takes the role of the *antenna*. Subsequent relaxation within the excited states of the ligand and then the ligand-to-metal energy transfer is what realizes the *antenna effect*.

Fig. 3 (b) presents the emission spectra of the complexes. A ligand to metal energy transfer process is observed for all the complexes. In fact, upon excitation involving the organic ligands (around 300 nm for all the complexes), the emission of Tb-based compounds consists of strong characteristic lines originating from the $^5D_4$ state of Tb(III) and in the case of Eu-based complexes from the $^5D_0$ state of Eu(III). Furthermore, we do not observe emission from the higher lying states $^5D_3$ and $^5D_{1,2,3}$ for Tb(III) and Eu(III), respectively, due to fast multiphonon relaxation to the aforementioned emissive levels.

As for excited state decay kinetics, it is interesting to underline that the decay time of $^5D_4$ level in **L2**Tb(NO$_3$)$_3$ (around 1 ms) is longer than the one of **L1**Tb(NO$_3$)$_3$ (around 0.2 ms) (Fig. S4). This is apparently strange, since the presence of NH vibrations, able to activate an efficient multiphonon relaxation process, should dominate the non-radiative quenching of the $^5D_4$ level. Since only **L2** ligand contains a NH group, **L2**Tb(NO$_3$)$_3$ would be expected to have a decay time shorter than the one of **L1**Tb(NO$_3$)$_3$. Therefore, the observed opposite trend could be due to the presence in **L1**Tb(NO$_3$)$_3$ of a competing non-radiative mechanism able to significantly quench the Tb(III) $^5D_4$ excited state. Such mechanism could be metal to ligand energy transfer (Back Transfer = BT) involving the ligand triplet state. In order to gain more insight into the energy transfer phenomena [triplet (T$_1$) to f* (T$_1 \rightarrow$ f*) or singlet (S$_1$) to f* (S$_1 \rightarrow$ f*) energy transfer process], we should first localize the energy of S$_1$ and T$_1$ levels for the **L1** and **L2** ligands. The approximate values of the S$_1$ and T$_1$ energies can be estimated from the fluorescence and phosphorescence spectra of **L1**Gd(NO$_3$)$_3$ and **L2**Gd (NO$_3$)$_3$ [16]. These data are reported in Table 1.

Since the optimal ΔE [T$_1$(S$_1$)-f*] should be small but large enough to minimize the back-energy transfer (BT) phenomenon, we can estimate the energy value of T$_1$ (or S$_1$) for an optimal energy transfer process. According to Heffern et al. [21] this energy is given by E(T$_1$/S$_1$) = 20400 (energy of $^5D_4$) + 1850 cm^{-1} = 22250 cm^{-1} for Tb(III) and 17200 (energy of $^5D_0$) + 1850 cm^{-1} = 19000 cm^{-1} for Eu(III).

The **L1** ligand has a T$_1$ energy close to the energy of $^5D_0$ of Eu(III) but significantly lower than $^5D_4$ of Tb(III). Therefore, in **L1**Tb(NO$_3$)$_3$ a metal to ligand energy transfer (BT) process is expected to take place; this is in agreement with the above discussion on the decay kinetics. Nevertheless, the presence of Tb(III) emission is observed under excitation into the ligands levels, reflecting an existence of ligand-to-Tb energy transfer, maybe involving the S$_1$ level of **L1** (21739 cm^{-1}). Also **L2** ligand has a value of T$_1$ energy lower than the $^5D_4$ but a BT process does not seem to occur or to occur only marginally. Following the spin selection rules, the most probable mechanism governing the non-radiative energy transfer involving the triplet state of the ligand and the f excited states of lanthanide ions, is the exchange mechanism [23]. The efficiency of this process can be evaluated only upon accurate determination of some variables, such as: i) energy overlap of the absorption and emission bands of the acceptor (A) and donor (D) ii) the D-A distance and iii) overlap and orientation of the orbitals involved in the mechanism [23]. Since this would require a detailed theoretical study, that is beyond the scope of the present contribution, in a future paper we will deal with the efficiency of the $^5D_4$ to T$_1$ BT mechanism, in the case of **L2** ligand. On the other hand, since the energy of the S$_1$ level of **L2** is optimal to transfer energy to Tb(III) (i.e. 22727 cm^{-1}), we can reasonably propose that the S$_1 \rightarrow$ f* ET is responsible for the antenna effect. It should be also noted that the T$_1$ energy of **L2** ligand is optimal for ET to Eu(III).

Luminescence emission spectra of the complexes containing **L1** and **L2** ligands, obtained at different pressures are presented in Fig. 4. The intensity of luminescence decreases with increasing pressure and it is completely quenched above the highest pressure presented in Fig. 4. This effect is accompanied by shortening of the luminescence decay times (Fig. S5). The pressure-induced red shift of individual peaks is negligible. One can notice that in the case of Eu(III) complexes samples under pressure an increase in intensity of the 582 nm line ($^5D_0 \rightarrow {}^7F_0$) is observed, in particular for **L2**Eu(NO$_3$)$_3$ (Fig. 4a).

Fig. S5 presents decay curves of the aforementioned complexes under different pressures. Luminescence decays are monitored at 545–550 nm corresponding to the $^5D_4 \rightarrow$ F$_5$ transition of Tb(III) and at 620 nm corresponding to the $^5D_0 \rightarrow {}^7F_2$ transition of Eu(III). Decays are non-exponential and it is clearly seen that the decay time decreases under pressure for all samples. Average values [τ_{avg}] of the time constant were determined using:

$$\tau = \frac{\int t \cdot I(t) dt}{\int I(t) dt}$$

where *I(t)* represents the emission intensity at time t. The obtained values are plotted against pressure in Fig. 5.

Contrary to the Tb(III)-based complexes discussed above, the τ_{avg} recorded at ambient pressure for the amine-based **L2**Eu(NO$_3$)$_3$ complex is significantly lower than the one recorded for **L1**Eu(NO$_3$)$_3$ (Fig. 5). In this case, it is reasonable to assume that, at ambient pressure, the main radiationless channel depopulating the $^5D_0$ excited level of Eu(III) is activated by the multiphonon relaxation process induced by the presence of NH vibrations in **L2**Eu(NO$_3$)$_3$. In addition, for this complex the

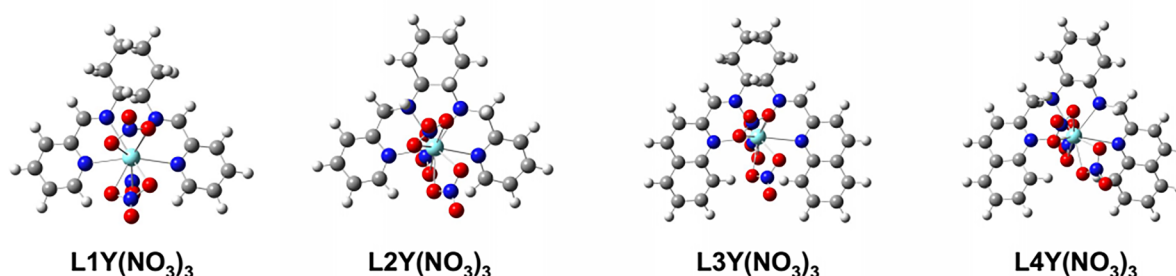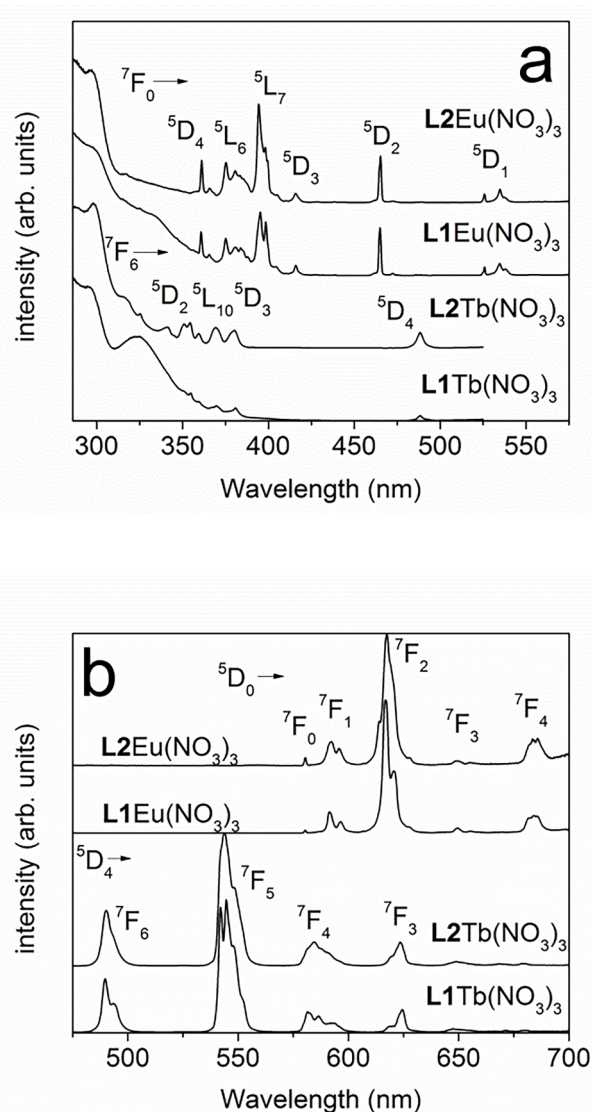**L1Y(NO$_3$)$_3$**   **L2Y(NO$_3$)$_3$**   **L3Y(NO$_3$)$_3$**   **L4Y(NO$_3$)$_3$**

Fig. 2. Optimized DFT molecular structures of Y complexes containing **L1**, **L2**, **L3** and **L4** ligands.

Fig. 3. Room temperature excitation (a) and emission (b) spectra of the complexes under investigation. Excitation spectra were monitored at 545 nm (for Tb-based complexes) corresponding to the $^5D_4 \rightarrow {}^7F_5$ transition in Tb(III) and 620 nm (for Eu-based complexes) corresponding to the $^5D_0 \rightarrow {}^7F_2$ transition in Eu(III). Emission spectra were excited at 300 nm.

Table 1
Barycenter of singlet (S_1) and triplet (T_1) excited states for ligands **L1** and **L2**. Data taken from Ref. [16].

Ligand	S_1 barycenter (cm^{-1})	T_1 barycenter (cm^{-1})
L1	21739	18220
L2	22727	19100

decrease of the lifetime upon increasing the pressure is very small (τ_{avg} is still around 0.2 ms at 150 kbar) although the emission intensity (upon excitation in the ligand band absorption bands) decreases significantly above 150 kbar. On the contrary, for all the other complexes both the decrease of the lifetimes and emission intensity are pronounced. The observed changes in luminescence (decrease of both the intensity and decay time) at high pressures can be interpreted considering two main aspects: i) since high pressure has a stronger influence on the singlet and triplet levels of the ligands than on the 4f levels of the lanthanide ions, the weakening of the luminescence efficiency with the pressure could be mainly due to a decreasing rate of the $T_1(S_1) \rightarrow f^*$ energy
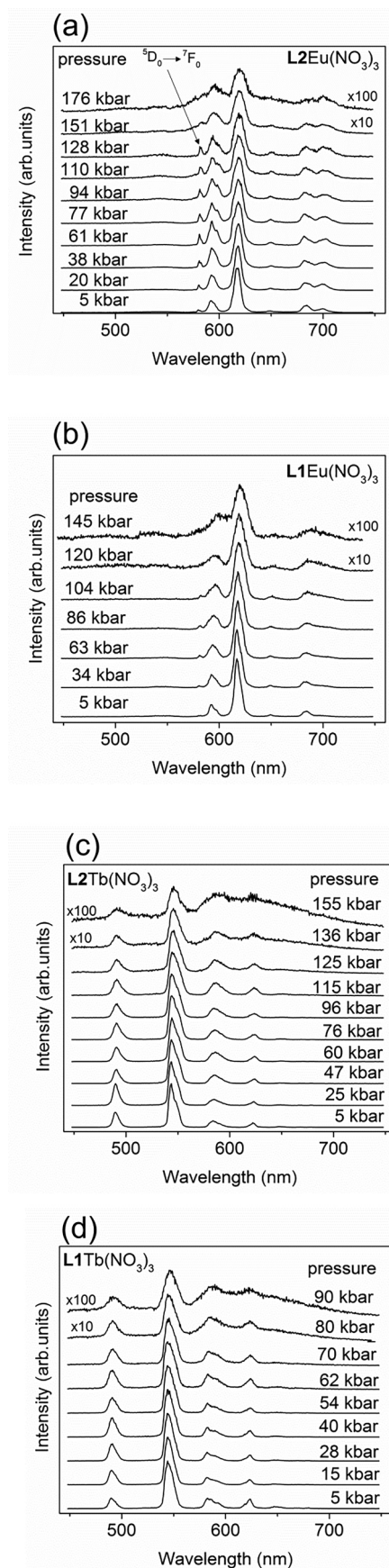
Fig. 4. Luminescence spectra of (a) **L2**Eu(NO$_3$)$_3$, (b) **L1**Eu(NO$_3$)$_3$, (c) **L2**Tb (NO$_3$)$_3$ and (d) **L1**Tb(NO$_3$)$_3$ obtained upon different pressures. The samplea were excited at 300 nm.
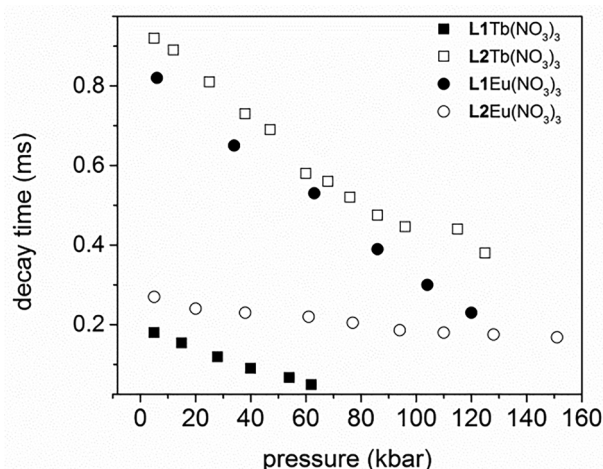
Fig. 5. Pressure dependence of the average decay time of Eu(III) in $L1Eu(NO_3)_3$ and $L2Eu(NO_3)_3$ and Tb(III) in $L1Tb(NO_3)_3$ and $L2Tb(NO_3)_3$.

Fig. 6. Luminescence spectra and decay curves of $L3Eu(NO_3)_3$ and $L4Eu(NO_3)_3$ obtained upon different pressures. Sample was excited with wavelength excitation 330 nm.

transfer, probably due to a decrease in energy of the ligands levels upon increasing the hydrostatic pressure. In this way, the T_1 level, for example, may not have the optimal energy to give an efficient ET process and, at the same time, BT mechanism could start to occur; ii) although less pronounced and probably negligible, the energy of the Ln(III) localized states could change with respect to the molecular orbitals (HOMO and LUMO) with increasing pressure. This may cause degeneration the excited f states of lanthanides with LUMO. The process of quenching of the luminescence intensity upon high pressure has been observed for Tb(III) in solids due to the degeneration of excited states with conduction band. On the other hand, non-radiative relaxation changes due to pressure-induced increases of vibrational energies are expected to be small, as energies of selected and representative modes increase by approximately $+ 0.1$ to $+ 0.7 \, cm^{-1}$/kbar [24]. As discussed above, the energy of T1 for L2 ligand is optimal to transfer energy to Eu(III) at ambient pressure. The probable decrease in energy of the ligand electronic levels upon compression is responsible of the worsening of the *antenna effect* even though BT process seems to occur only marginally. On the other hand, the effect of the pressure brings the T1 (and S_1) energy significantly below the energy of $^5D_4$ level of Tb(III), activating a BT mechanism in $L2Tb(NO_3)_3$ complex. By means of a similar reasoning, it is possible to explain the decrease of both lifetimes and emission intensities upon increasing the pressure, in the cases of L1-based complexes.

3.2.2. Quinoline-based complexes

As for the lanthanide complexes containing the quinoline-based ligands (L3 and L4) are concerned, the excitation of Tb(III) (direct and through antenna effect) does not produce any detectable emission from the metal ion in $L3Tb(NO_3)_3$ and a very weak one from $L4Tb(NO_3)_3$ at ambient pressure. For this reason, these complexes were not examined under high hydrostatic pressure. Luminescence excitation spectra of $L3Eu(NO_3)_3$ monitored at 615 nm, i.e. corresponding to the $^5D_0 \rightarrow {}^7F_2$ emission transition of Eu(III) consists of a broad band with maximum at about 330 nm and very weak sharp lines associated with the f-f transitions from the ground state to the excited states of the Eu(III) ion (Fig. S6). Also for this complex an efficient sensitization of Eu(III) luminescence is possible by involving orbitals localized on the ligand [L3Y(NO_3)_3, Fig. S2]. The spectrum of $L4Eu(NO_3)_3$ consists of two broad bands with maxima at 325 nm and 370 nm (Fig. S6). Luminescence spectra of $L3Eu(NO_3)_3$ and $L4Eu(NO_3)_3$ obtained at different pressures are presented in Fig. 6.

The intensity of luminescence decreases with increasing pressure and it is completely quenched at above the highest pressure presented in Fig. 6. Pressure-induc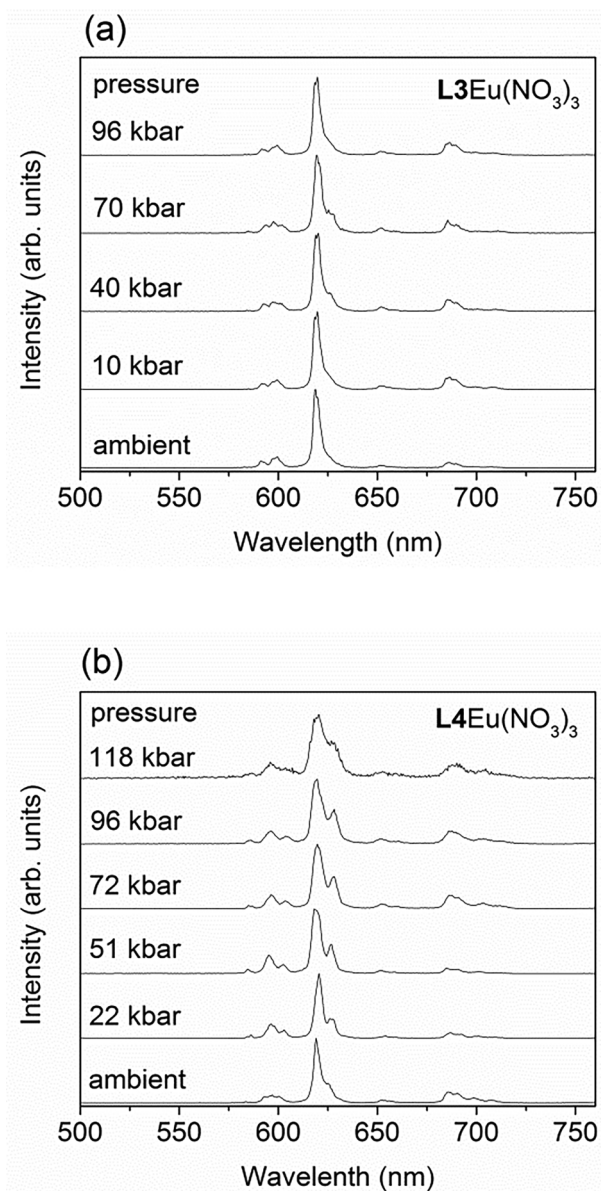ed red shift of individual peaks is negligible. In the case of $L4Eu(NO_3)_3$, a broaderning and a change in splitting of $^5D_0 \rightarrow {}^7F_2$ transition is observed. The increase of the linewidth with increasing pressure is related to the increase of inhomegeneous broadening induced by pressure. Decays are non-exponential and it is clearly seen that the decay time, monitored at 615 nm corresponding to the $^5D_0 \rightarrow {}^7F_2$ transition of Eu(III) (Fig. S7), decreases under pressure for $L3Eu(NO_3)_3$ and does not change or decrease slightly for $L4Eu(NO_3)_3$. The obtained values of τ_{avg} are plotted against pressure in Fig. 7.

As for $L2Eu(NO_3)_3$ complex, also in the case of $L4Eu(NO_3)_3$ the decrease of luminescence intensity with increasing the pressure is not accompanied by a decrease of lifetimes. For both complexes, by changing the pressure additional non-radiative quenching of the $^5D_0$ level seem to occur only marginally and the pressure-induced increase of multiphonon relaxation is not significant. This behavior is peculiar to each Eu(III) complex containing the amine-based ligands L2 and L4 and seems to be connected with the energy of the triplet state (T1), which is similar for the two ligands [19100 cm^{-1} (L2) and 19200 cm^{-1} (L4);
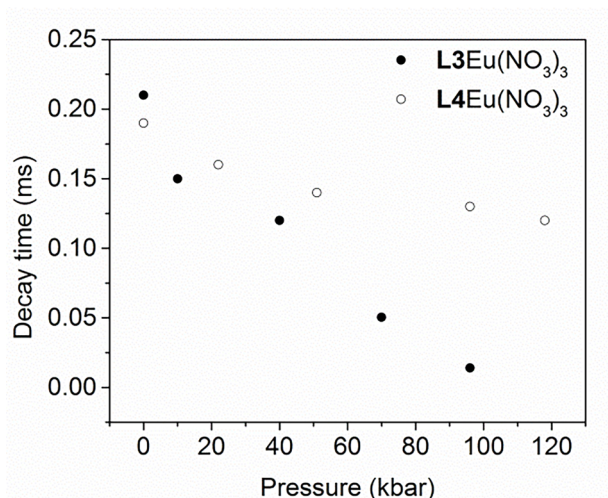
Fig. 7. Pressure dependence of the average decay time of Eu(III) in **L3**Eu(NO$_3$)$_3$ and **L4**Eu(NO$_3$)$_3$.

data taken from the phosphorescence spectra of the respective Gd complexes [16,17,22] and it is optimal to sensitize Eu(III) luminescence. The pressure-induced decrease of the energy of the **L2** and **L4** electronic levels is not sufficient to activate a BT mechanism from the metal ion to the ligand.

4. Conclusions

In this contribution, the luminescence spectroscopy of Eu(III) and Tb(III) complexes of imine-based (**L1** and **L3**) and amine-based (**L2** and **L4**) ligands has been investigated under high hydrostatic pressure. In all cases, the emission intensities decrease upon increasing the pressure. This is accompanied by a concomitant reduction of the luminescence decay times of $^5D_0$ Eu(III) and $^5D_4$ Tb(III) excited states, for all the Tb-based complexes and for the imine-based complexes of Eu(III). In these cases, non-radiative back energy transfer process (from the metal to the ligand) shall be considered as dominating mechanism responsible for the reduction of the luminescence efficiency. On the contrary, in the case of amine-based Eu(III) complexes [**L2**Eu(NO$_3$)$_3$ and **L4**Eu(NO$_3$)$_3$] a very small reduction of the decay times is noticed. Both **L2** and **L4** ligands present triplet states whose energy is optimal to sensitize Eu(III) luminescence [almost 2000 cm^{-1} above the energy of $^5D_0$ level of Eu (III)]. The pressure-induced decrease of the energy of the electronic levels of the ligands worsens the ligand to metal energy transfer efficiency but is not sufficient to activate the back energy transfer process (from the metal to the ligand). All this results in a reduction of the Eu (III) emission intensities upon ligand excitation and a negligible

reduction of $^5D_0$ Eu(III) excited state lifetime. Finally, thanks to the DFT calculations we were able to understand the nature of the NTO orbitals involved in the main UV electronic absorption transitions upstream of the energy transfer process to the metal ion. For all the complexes, these transitions correspond to a locally-excited (LE) process.

Appendix A. Supplementary data

Supplementary data to this article can be found online at https://doi.org/10.1016/j.ica.2019.119179.

References

[1] J.C.G. Bünzli, Chem. Rev. 110 (2010) 2729–2755.
[2] H. Tsukube, S. Shinoda, Chem. Rev. 102 (2002) 2389–2404.
[3] S.J. Butler, D. Parker, Chem. Soc. Rev. 42 (2013) 1652–1666.
[4] J.C.G. Bünzli, S.V. Eliseeva, Chem. Sci. 4 (2013) 1939–1949.
[5] M.C. Heffern, L.M. Matosziuk, T.J. Meade, Chem. Rev. 114 (2014) 4496–4539.
[6] J.W. Walton, A. Bourdolle, S.J. Butler, M. Soulie, M. Delbianco, B.K. McMahon, R. Pal, H. Puschmann, J.M. Zwier, L. Lamarque, O. Maury, C. Andraud, D. Parker, Chem. Commun. 49 (2013) 1600–1602.
[7] J.M. Stanley, X. Zhu, X. Yang, B. Holliday, J. Inorg. Chem. 49 (2010) 2035–3037.
[8] K.S. Kisel, G. Linti, G.L. Starova, V.V. Sizov, A.S. Melnikov, A.P. Pushkarev, M.N. Bochkarev, E.V. Grachova, S.P. Tunik, Eur. J. Inorg. Chem. (2015) 1734–1743.
[9] S.K. Behzad, M.M. Amini, M. Ghanbari, M. Janghouri, P. Anzenbacher Jr., S.W. Ng, J. Kido, Y. Okamoto, Chem. Rev. 102 (2002) 2357–2368.
[10] Y. Luo, Z. Liu, H.T. Wong, L. Zhou, K.-L. Wong, K.K. Shiu, P.A. Tanner, Adv. Sci. 6 (2019) 1900487–1919059.
[11] M.M. Nolasco, P.M. Vaz, V.T. Freitas, P.M. Lima, P.S. Andrè, R.A.S. Ferreira, P.D. Vaz, P. Ribeiro-Claro, L.D.J. Carlos, Mater. Chem. A 1 (2013) 7339–7350.
[12] X. Wang, T. Wang, X. Tian, L. Wang, W. Wu, Y. Luo, Q. Zhang, Sol. Energy 85 (2011) 2179–2184.
[13] A. Gavriluta, T. Fix, A. Nonat, A. Paire, L. Slaoui, L.J. Charbonnière, Guillemoles J.-F Adv. Opt. Mat. 4 (2016) 1846–1853.
[14] A. de Bettencourt-Dias, P.S. Barber, S. Viswanathan, Coord. Chem. Rev. 273–274 (2014) 165–200.
[15] A.V. Hayes, H.G. Drickamer, J. Chem. Phys. 76 (1) (1982) 114–125.
[16] M. Mihorianu, M. Leonzio, M. Bettinelli, F. Piccinelli, Inorg. Chim. Acta 438 (2015) 10–13.
[17] M. Mihorianu, M. Leonzio, M. Monari, L. Ravotto, P. Ceroni, M. Bettinelli, F. Piccinelli, Chem. Select 1 (2016) 1996–2003.
[18] T. Yanai, D.P. Tew, N.C. Handy, Chem. Phys. Lett. 393 (2004) 51–57.
[19] M.J. Frisch, G.W. Trucks, H.B. Schlegel, G.E. Scuseria, M.A. Robb, J.R. Cheeseman, G. Scalmani, V. Barone, B. Mennucci, G.A. Petersson, et al., Gaussian 09, Revision D.01, Gaussian, Inc., Wallingford CT, 2013.
[20] R.L. Martin, J. Chem. Phys. 118 (2003) 4775–4777.
[21] M.C. Heffern, L.M. Matosziuk, T.J. Meade, Chem. Rev. 114 (2014) 4496–4539.
[22] F. Piccinelli, A. Speghini, M. Monari, M. Bettinelli, Inorg. Chim. Acta 385 (2012) 65–72.
[23] D.L. Dexter, J. Chem. Phys. 21 (1953) 836–850.
[24] Y. Suffren, F.-G. Rollet, C. Reber, Comments Inorg. Chem. 32 (2011) 246–276.